

Comparison of Acid Mine Drainage Microbial Communities in Physically and Geochemically Distinct Ecosystems

PHILIP L. BOND,* GREG K. DRUSCHEL, AND JILLIAN F. BANFIELD

Department of Geology and Geophysics, University of Wisconsin, Madison, Wisconsin 53706

Received 27 March 2000/Accepted 29 August 2000

This study presents population analyses of microbial communities inhabiting a site of extreme acid mine drainage (AMD) production. The site is the inactive underground Richmond mine at Iron Mountain, Calif., where the weathering of a massive sulfide ore body (mostly pyrite) produces solutions with pHs of ~0.5 to ~1.0. Here we used a suite of oligonucleotide probes, designed from molecular data recently acquired from the site, to analyze a number of microbial environments by fluorescent in situ hybridization. Microbial-community analyses were correlated with geochemical and mineralogical data from those environments. The environments investigated were within the ore body and thus at the site of pyrite dissolution, as opposed to environments that occur downstream of the dissolution. Few organism types, as defined by the specificities of the oligonucleotide probes, dominated the microbial communities. The majority of the dominant organisms detected were newly discovered or organisms only recently associated with acid-leaching environments. “*Ferroplasma*” spp. were detected in many of the communities and were particularly dominant in environments of lowest pH and highest ionic strength. *Leptospirillum* spp. were also detected in many slime and pyrite-dominated environments. In samples of an unusual subaerial slime, a new uncultured *Leptospirillum* sp. dominated. *Sulfobacillus* spp. were detected as a prominent inhabitant in warmer (~43°C) environments. The information gathered here is critical for determining organisms important to AMD production at Iron Mountain and for directing future studies of this process. The findings presented here also have relevance to the microbiology of industrial bioleaching and to the understanding of geochemical iron and sulfur cycles.

We have investigated microbial and geochemical characteristics of the extreme acid mine drainage (AMD) site at Iron Mountain, Calif. (15, 32, 36). At this location, extensive mining by underground tunneling and blasting has exposed a massive sulfide ore body, comprised of approximately 95% pyrite (FeS₂), to weathering by water and air (27). Dissolution of the pyrite ore body results from oxidation and produces acid according to the reaction $\text{FeS}_2 + 14\text{Fe}^{3+} + 8\text{H}_2\text{O} \rightarrow 15\text{Fe}^{2+} + 2\text{SO}_4^{2-} + 16\text{H}^+$ (26). The water discharged from the mine is treated to neutralize the drainage and precipitate metals before the water is released into the Keswick reservoir.

Chemolithotrophic prokaryotes such as *Acidithiobacillus ferrooxidans* (formerly known as *Thiobacillus ferrooxidans* [24]) and *Leptospirillum ferrooxidans* are known to enhance acid production in metal-leaching environments by oxidizing Fe²⁺ and replenishing the oxidant Fe³⁺ (34). To better understand details of microbially enhanced pyrite oxidation, much attention has been placed on characterizing *A. ferrooxidans* and *L. ferrooxidans*. However, acid-leaching environments support a diverse range of iron- and sulfur-oxidizing chemolithotrophs as well as heterotrophic microorganisms (22). Indeed, investigations of microbial communities by fluorescent in situ hybridization (FISH) indicate that *A. ferrooxidans* and *L. ferrooxidans* are not the predominant microorganisms in regions where the pyrite ore body is located at the Iron Mountain mine (15, 36). In those studies it was found that *A. ferrooxidans* was prominent in higher-pH solutions downstream from the pyrite ore (15, 36). However, these prior studies did not resolve what the predominant organisms are in the lower-pH regions at the site. In fact, distributions and associations of acidophiles and the

influence of geochemical conditions in acid-leaching environments are far from thoroughly investigated.

Within the Richmond mine, where the ore body is located, four tunnels (termed drifts) branch away from the entrance tunnel at a location called the five-way junction or simply the five-way (Fig. 1). Water flows over and through pyrite sediment in the tunnels, collects at the five-way, and is piped out of the mine for treatment (Fig. 1). There are obvious macroscopic forms of microbial biomass occurring in the flowing water. These include submerged slime streamers attached to the sediment (Fig. 2A) and slimes on the water surface. Other visible microbial growths occur as subaerial slimes and as pendulous slime stalactites dripping from the mine tunnel ceilings and walls (Fig. 2B). In addition to eye-visible slimes, surfaces of pyrite grains are often covered by microbial cells.

To better understand the acid production, we have characterized the microbiology of samples from the Iron Mountain mine in the five-way region, where pyrite actively dissolves. The pH of water at the five-way typically ranges from ~0.5 to ~1.0. However, more-extreme values (as low as -3.6) have been reported from concentrated solutions deeper in the mine (27).

Molecular investigations reveal that microbial communities occurring in solutions and sediments within the ore body are made up mostly of organisms that have not yet been cultured although they are phylogenetically related to known acidophiles. 16S rRNA cloning studies have revealed the presence of novel organisms from the *Leptospirillum*, *Thermoplasmatales*, *Sulfobacillus*, *Acidimicrobium*, and *Acidiphilium* groups (7, 16). We have recently divided the expanded *L. ferrooxidans* cluster of 16S rRNA sequences into three groups which may represent different genera (7). The results of our molecular studies contrast to those of other investigations, suggesting that microbial populations from highly acidic metal-leaching environments are dominated by previously cultured organisms (19, 39).

* Corresponding author. Present address: School of Biological Sciences, University of East Anglia, Norwich NR4 7TJ, United Kingdom. Phone: (44 1603) 593534. Fax: (44 1603) 592250. E-mail: phil.bond@uea.ac.uk.

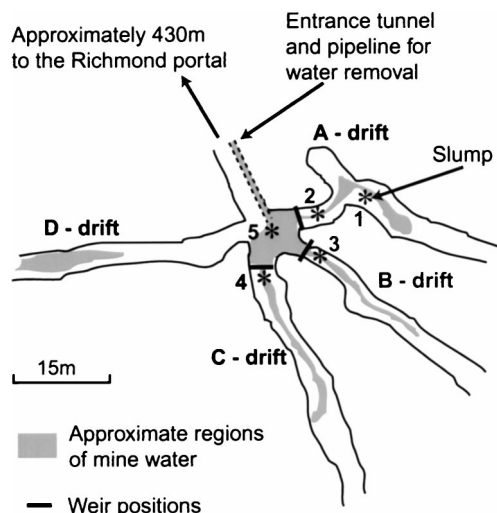


FIG. 1. Schematic map of the Richmond five-way section of the mine. Asterisks mark locations of environmental measurements and sampling, and the numbers correspond to sample descriptions (Table 2).

In situ hybridization analysis (with a genus-specific probe, FER656 [14]) shows that a slime located in the B drift is dominated by a novel iron-oxidizing archaeon belonging to the genus "*Ferroplasma*" (the quotes indicate that this is not a recognized name). Thus, it is clear that the recently discovered organisms are important in the production of AMD at Iron Mountain. However, it is apparent that there are different microbial assemblages occurring in different environments within the ore body regions of the mine. This is indicated by visible macroscopic differences and conclusively verified by community analyses performed by cloning DNA and FISH (6, 7).

We have designed oligonucleotide probes for the detection of prominent organisms that possibly facilitate dissolution at Iron Mountain (see Table 1) (6). These include a new probe that detects uncultured *Leptospirillum* group III spp. (6). This group would not have been detected with the previously used *L. ferrooxidans* group probe (36). Preliminary testing indicates that we can identify by FISH, at the genus and subgenus level, the majority of organisms in samples from the Iron Mountain mine (6). The next phase of these investigations is to quantitatively survey microbial communities within the mine using the newly developed oligonucleotide probes. This study reports detailed analyses of microbial communities occurring in various mine low-pH environments in the context of the prevailing geochemical and mineralogical conditions.

MATERIALS AND METHODS

The study site, environmental measurements, and sample collection. A general description of the Richmond mine site at Iron Mountain is provided elsewhere (15). In this study we restricted sample locations to regions of the mine that occur within the sulfide ore body (Fig. 1). The groundwater in these regions has pH values between 0.5 and 1.0. In contrast, water flowing from the mine peripheral to the ore body (e.g., in the entrance tunnel and in drainage streams) has pH values between 2 and 4.

Sample collection and environmental measurements were carried out in November 1998 and in February, May, and October 1999. Conductivity, pH, and temperature measurements were carried out as described previously (15). Samples for FISH analyses of biofilms and sediments were collected and fixed in paraformaldehyde as described previously (6). For mineralogical analyses, samples of corresponding sediment were collected into sterile 15-ml Falcon tubes.

Mine solution total iron and ferrous iron concentrations were determined on site, in samples collected in May 1999, by the FerroZine and phenanthroline

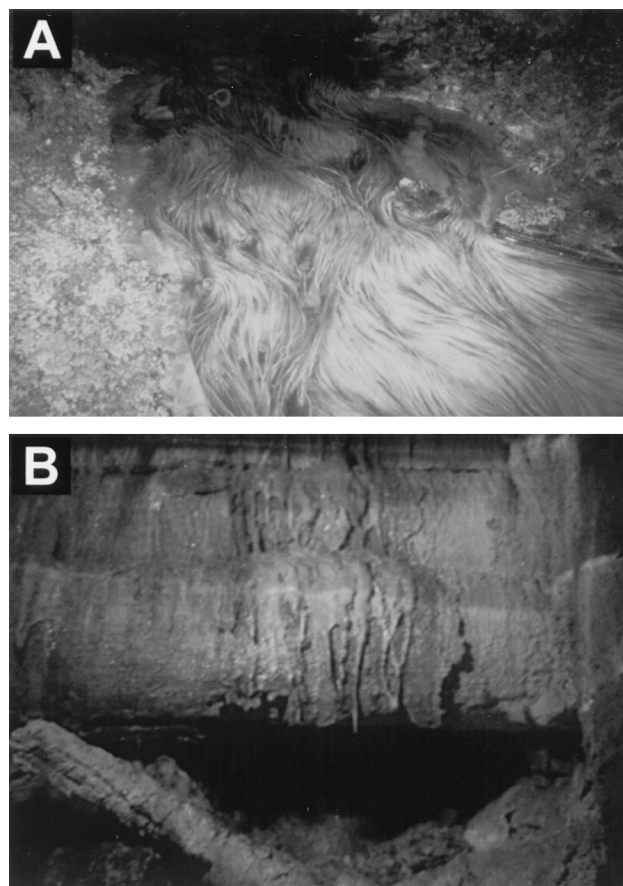


FIG. 2. Images of biofilm material present at the Iron Mountain mine. (A) Submerged slime streamers (biofilm) in a B-drift stream (approximately 1 m across) that are anchored to the sediment. The three drifts sampled all had macroscopically similar slime streamers. Reprinted with permission from the American Association for the Advancement of Science (14) (<http://www.sciencemag.org>). (B) Pendulous biofilms (termed snottites) hanging from the tunnel wall directly above the slump in the A drift.

methods (HACH DR/2010 spectrophotometer methods 8147 and 8146), respectively.

Mineralogy. Sediment samples were ground in a mortar and pestle, suspended in ethanol (EtOH), and mounted on glass slides. The samples were analyzed on a Scintag PADV X-ray diffractometer over a 2-theta range of 10 to 80 degrees. Minerals were identified by comparison with minerals in the JCPDS database. Sediment samples were also digested with 30% hydrogen peroxide to dissolve all sulfide material; the resulting solution was then analyzed on a Dionex Series 500 ion chromatography system equipped with a UV detector. The ion chromatography method was adapted from Dionex technical note 10 (1999), and the Fe, Zn, Pb, and Cu concentrations of the samples were determined. The proportions of silicate and sulfide material were determined by visual estimation of modal abundances from several sample splits.

Whole-cell hybridization and fluorescent microscopy. The fixed biofilm samples were homogenized and spotted onto gelatin-coated multiwell slides and dehydrated as described previously (6). The fixed sediment sample was a subsample of the fixed biofilm sample (B-drift slime). This subsample was obtained by homogenizing the original biofilm sample and then removing the supernatant containing most of the associated biofilm. The remaining sediment was then washed and resuspended in the fixed-cell storage buffer (6). Sediment samples were then spotted onto gelatin-coated multiwell slides, dried, and dehydrated.

Oligonucleotide probes used in this study were synthesized and labeled with Cy3, as described previously (6). Many of these probes are specific for AMD organisms detected at the Iron Mountain mine (Table 1). For FISH, the dehydrated fixed samples were hybridized with oligonucleotide probes and then stained with DAPI (4',6'-diamidino-2-phenylindole) under the conditions previously described (6).

Samples were examined by light microscopy and for fluorescent signals from FISH and DAPI using a Leica LEITZ DMRX epifluorescence microscope as described previously (6). Images were captured with a Hamamatsu digital

TABLE 1. 16S rRNA-targeted oligonucleotide probes used in this study

Probe name	Specificity	Sequence (5'-3')	Reference
UNIV1392	All organisms (universal)	ACGGGCGGTGTGTRC	29
EUK502	Eukaryote domain	ACCAGACTTGCCCTCC	2
EUB338	Bacterial domain	GCTGCCTCCCGTAGGAGT	2
ARCH915	Archaeal domain	GTGCTCCCCCGCCAATTCCT	37
NON338	No target (control for nonspecific binding)	ACTCCTACGGGAGGCAGC	38
LF581	<i>Leptospirillum</i> groups I and II	CGGCCTTTACCAAAGAC	36
LF1252	<i>Leptospirillum</i> group III	TTACGGGCTCGCCTCCGT	6
LF655	<i>Leptospirillum</i> groups I, II, and III	CGCTTCCCTCTCCCAGCCT	6
SUL228	<i>Sulfobacillus thermosulfidooxidans</i>	TAATGGGCGCGAGCTCCC	6
FER656	" <i>Ferroplasma</i> " genus	CGTTTAACCTCAGCCGATC	14
TH1187	<i>Thermoplasmales</i> group	GTACTGACCTGCCGTGCAGC	6
THC642	<i>Acidithiobacillus caldus</i>	CATACTCCAGTCAGCCCGT	13
TF539	<i>Acidithiobacillus ferrooxidans</i>	CAGACCTAACGTACCGCC	36
ACM732	<i>Acidimicrobium</i> and relatives	GTACCGGCCAGATCGCTG	6
ACD840	<i>Acidiphilium</i> genus	CGACACTGAAGTGCTAAGC	6
SRB281	Various δ - <i>Proteobacteria</i>	TCAGACCAGCTAACCATC	6

charge-coupled-device camera using Axiovision software, converted to gray-scale PICT files in Adobe Photoshop 5.0, and compiled in Adobe Illustrator 7.0. To enumerate, the DAPI-stained cells detected with probes were counted individually for each probe on each of the samples. Probe signal counts were made prior to DAPI signal counts to avoid quenching of the probe signal. For each probing event, between 800 and 1,200 DAPI-stained cells were counted for the biofilm cell counts and between 188 and 830 cells were counted for the sediment-attached cells. Enumerations were made from at least 16 microscope fields, taken from no less than four different wells (on the multiwell slides). The estimated percentage of cells detected by the probe was the average percentage of the counted fields. The error bars presented in Fig. 4 represent the standard deviations for the sediment cell counts and twice the standard deviations for biofilm cell counts.

Electron microscopy. Samples were prepared for transmission electron microscopy (TEM) by glutaraldehyde fixation (2.5%) for 2 h. After three washes in phosphate-buffered saline (PBS), samples were incubated in osmium oxide (1%) for 1 h. Following three more PBS washes, the samples were gradually dehydrated in an EtOH series (30, 50, 75, and 95% EtOH in PBS; dehydrations were 15 min each). After a complete dehydration in three 100% EtOH washes, the samples were infiltrated with LR White embedding resin (50:50 with EtOH for 1 h). Then, after three more changes in LR White resin, these samples were embedded in gelatin capsules. The blocks were incubated at 60°C for 24 h and then sectioned on a Leica Ultra Cut S microtome to a 70-nm section thickness. Sections were mounted on Formvar and carbon-coated copper grids and stained with 2.5% uranyl acetate and 1% lead citrate. Grids were examined with a CM 200 UT Philips transmission electron microscope operated at 120 kV.

RESULTS

Sample locations. Ranges of sample locations and sample types were chosen to cover some of the geographical region and a range of the visibly different microbial growths that occur there.

Environmental measurements were taken from five loca-

tions within the mine. Three locations in the A, B, and C drifts, termed upper regions, were just upstream of drift weirs (see locations 2, 3, and 4 in Fig. 1). Another location was in the five-way junction near the water outlet pipe (location 5 in Fig. 1). The other location was at a slump that had formed in the A drift, termed the slump (location 1 in Fig. 1). Water was flowing through the A, B, and C drifts on all sampling occasions. Flowing water was not observed in the D drift.

Mine locations sampled for microbial-community analyses correspond to the positions where environmental measurements were made (Table 2). Slime streamers (Fig. 2A) were always present in drifts containing flowing water (A, B, and C drifts). Slime streamer samples together with associated sediment were taken from the B and C drifts during the visits for sample collection (locations 3 and 4 in Fig. 1). A slime layer on the water surface in the upper region of the A drift was sampled (location 2 in Fig. 1). At the other location, also in the A drift, a slump had formed on the tunnel floor (location 1 in Fig. 1). From this location, samples of subaerial slimes, formed on top of the slump, and biofilms hanging from the mine tunnel walls above the slump (previously termed snottites [7]) were taken (Fig. 2B). The slime streamer and subaerial slime samples contained abundant, fine-grained pyrite sediment.

Geochemical conditions. Solution temperature, pH, ionic strength, and dissolved-oxygen-content measurements were made at the five locations within the mine (Fig. 3). In general, the water temperature was highest in February and May. This corresponded to periods of highest water flow through the mine (data not shown). In all locations high conductivity cor-

TABLE 2. Sample description for microbial-community analysis

Sample name	Location in mine ^a	Physical description	Sample period(s)
Slump slime	On top of a slump that had formed (~1.5 m high) on the A-drift tunnel floor {1}	Thick (~1 cm) slime on the slump pyrite sediment; moist, gelatinous consistency	February 1999
Snottite	Directly above the slump in the A drift {1}	Slime dripping from tunnel wall and ceiling	February 1999
Surface slime	A-drift upper region {2}	Thin pink slime covering a large section of the water surface	February 1999
B-drift slime	B-drift upper region {3}	Submerged slime streamer attached to sediment	November 1998, October 1999
B-drift sediment	B-drift upper region {3}	Pyrite sediment particles separated from the B-drift slime	October 1999
C-drift slime	C-drift upper region {4}	Submerged slime streamer attached to sediment	February 1999, October 1999

^a Numbers enclosed by braces correspond to map locations in Fig. 1.

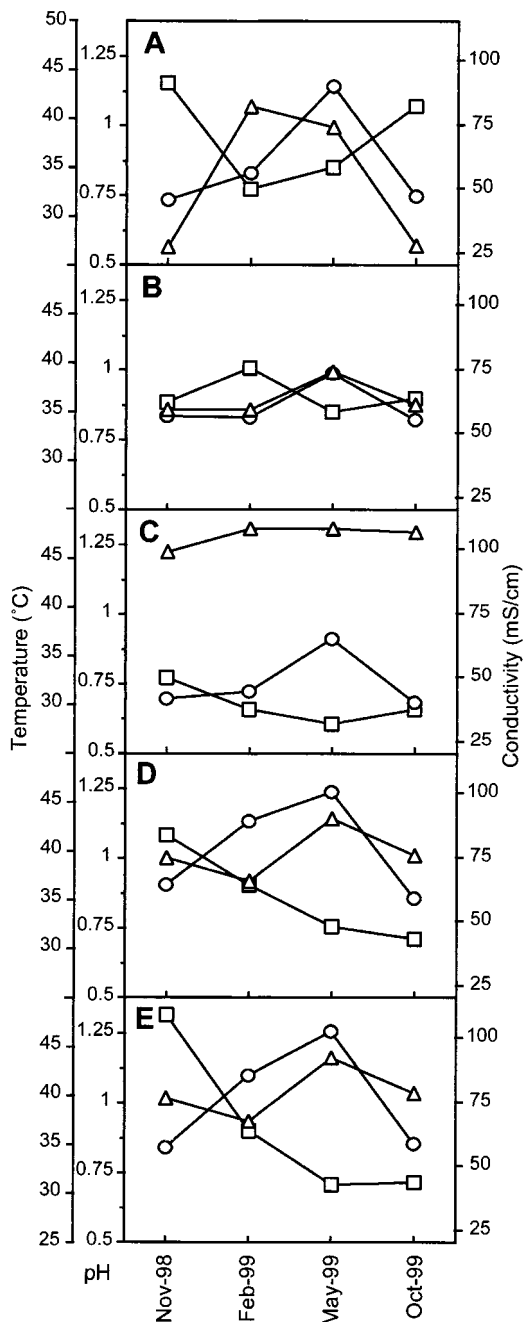


FIG. 3. Environmental conditions of pH (□), temperature (○), and conductivity (△) measured at the following sites: the A-drift slump (location 1) (A), the A-drift upper region (location 2) (B), the B-drift upper region (location 3) (C), the C-drift upper region (location 4) (D), and the discharge point (pipe entrance) at the Richmond five-way (location 5) (E). Refer to Fig. 1 for the location points of analytical measurements. Nov, November; Feb, February; Oct, October.

related with low pH values. The B-drift upper region always had the lowest pH. The C-drift upper region was consistently the warmest location, rising to 46°C in May 1999. Conditions in the C-drift upper region were most similar to those in the five-way, as ~85% of the total flow in the five-way comes from the C drift.

Total iron and ferrous iron concentrations were measured in solutions from locations 1 to 5 (Fig. 1). All solutions had high

total iron concentrations ranging from 20.95 to 23.48 g/liter. In these solutions, ferrous iron was the major species, making up 90.3 to 93.6% of the total iron.

Mineralogy. B-drift sediment contained approximately 90% pyrite, which had a typical diameter of <200 μm. Chromatographic determination of the transition metal content in the sulfide fraction measured about 2% Zn, 1% Cu, and no appreciable Pb. Silicate material was mostly quartz and plagioclase. Although B- and C-drift mineralogies were comparable, there were more silicates in the C drift (~25%) and the pyrite grain size was typically larger (up to several centimeters in diameter). Sediment collected from the slump in the A drift contained a significant proportion (up to 50% modal abundance) of an amorphous brown material identified by X-ray analysis as the ferric iron sulfate mineral jarosite, $KFe_3(SO_4)_2(OH)_6$. Well-formed crystals of K-Fe-sulfate with cubic symmetry (probably voltaite) were detected on pyrite surfaces by scanning electron microscopy.

Microbial-community analyses. Results of microbial-community analyses by FISH of eight different samples are shown in Fig. 4. In all samples, high proportions of the DAPI-stained cells were detected as the sum of the *Bacteria*- and *Archaea*-specific probe counts. Probe-detected cells totaled 65% in the snottite sample and above 79% for all other samples. As we have found on other occasions, high proportions of these communities contain rRNA levels that permit detection by FISH (6, 15, 36). Other probes, not noted in Fig. 4, were used for analysis of these samples, and results are mentioned below.

Examples of cells detected in some biofilms by FISH are shown (Fig. 5). These images were taken from regions where separated cells could be observed and do not fully convey the very high density of cell packing in these biofilms.

The probe NONEUB, which is complementary to probe EUB338, was used to determine nonspecific binding of the probe in samples. In all samples, only small amounts of nonspecific binding were detected and elucidation of this was possible only in the slump slime and the snottite samples (Fig. 4A and B).

A-drift communities. The slump slime and snottite samples contained thick masses of densely packed cells (estimated to range between $\sim 10^{10}$ and 10^{12} cells/g). In both samples, iron sulfate crystals were present and cells were attached to these. The slump slime also contained pyrite particles with attached cells. Both these biofilms contained similar microbial populations that were dominated by *Leptospirillum* group III cells, detected with probes LF655 and LF1252 (Fig. 4A and B). These were evident as curved rods and spirillum-shaped cells (Fig. 5A). *Acidimicrobium* spp. also made up considerable proportions of these communities. These were evident mostly as small rods that were scattered throughout the biofilm.

Although species of the delta subdivision of the *Proteobacteria* (δ -*Proteobacteria*) and *Thermoplasmatales* were previously detected by cloning community DNAs from these samples (7), cells could not be localized with probes SRB281 and TH1187, respectively. Eukaryotes in the form of large, unicellular, nucleus-containing organisms made up less than 1% of DAPI-stained cells (results not shown) and were tentatively identified as protozoa.

Some 15 and 35% of the cells in the slump slime and snottite samples, respectively, were not detected with the prokaryote probes, the eukaryote-specific probe, or the universal probe. When stained with DAPI, these appeared as small (<1-μm diameter) (Fig. 5A), brightly fluorescent (i.e., DNA-bearing), coccus-shaped cells. As cell permeability could hinder probe access to the rRNA, we tried FISH on samples after increasing cell permeability. Treatments included combinations of either

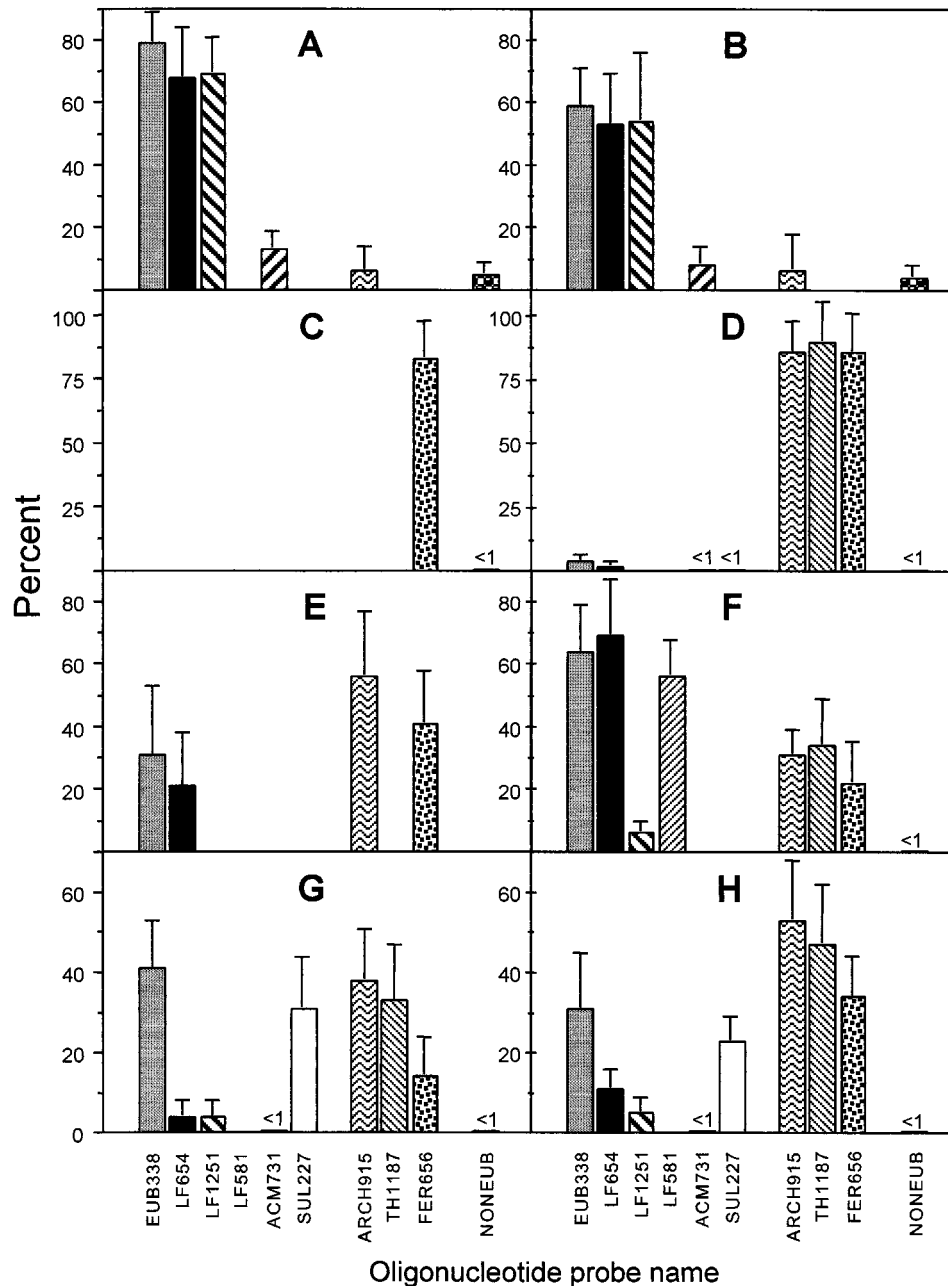


FIG. 4. Microbial-community analysis as determined by FISH cell counts on samples of the A-drift slump slime (A), A-drift snottite (B), B-drift slime (November 1998 sample) (C), B-drift slime (October 1999 sample) (D), B-drift sediment (October 1999 sample) (E), A-drift surface slime (F), C-drift slime (February 1999 sample) (G), and the C-drift slime (October 1999 sample) (H). The values obtained are expressed as percentages of the number of cells detected with the DAPI stain (see Materials and Methods). Only the positive portions of error bars are shown. Values shown as <1 were qualitative estimates only.

proteinase K (1 mg/ml) at 50°C for 40 min or lysozyme (5 mg/ml), urea (5 M), HCl (0.5 M), or sodium dodecyl sulfate (0.3%), all at 37°C for 1 h. However, no specific RNA probe binding was achieved.

To further investigate the nature of small cocci, samples were examined by TEM. In addition to the presence of spirilla and curved rods, TEM indicated that the slump slime and snottite biofilms contained many pleomorphic cocci ranging from 50 to 500 nm in diameter (Fig. 6A and B). The cocci were bounded by a single membrane and, in almost all cases, appeared to contain cytoplasm. Cells were often observed to be

in stages of budding or dividing (Fig. 6C). Structures identified as protein S-layers with hexagonal symmetry were also observed on a few of the larger cocci (Fig. 6D).

The other sample investigated from the A drift was a slime floating on the surface of the flowing mine solution. The slime was a three-dimensional biofilm of densely packed cells and was dominated by spirilla and curved rods that were mostly of the *Leptospirillum* group I and II types (Fig. 4F). *Archaea*, which made up 34% of the cells, were all of the *Thermoplasmales* order, and most of these were of the genus "*Ferroplasma*." As in the slump slime and snottite biofilms, eu-

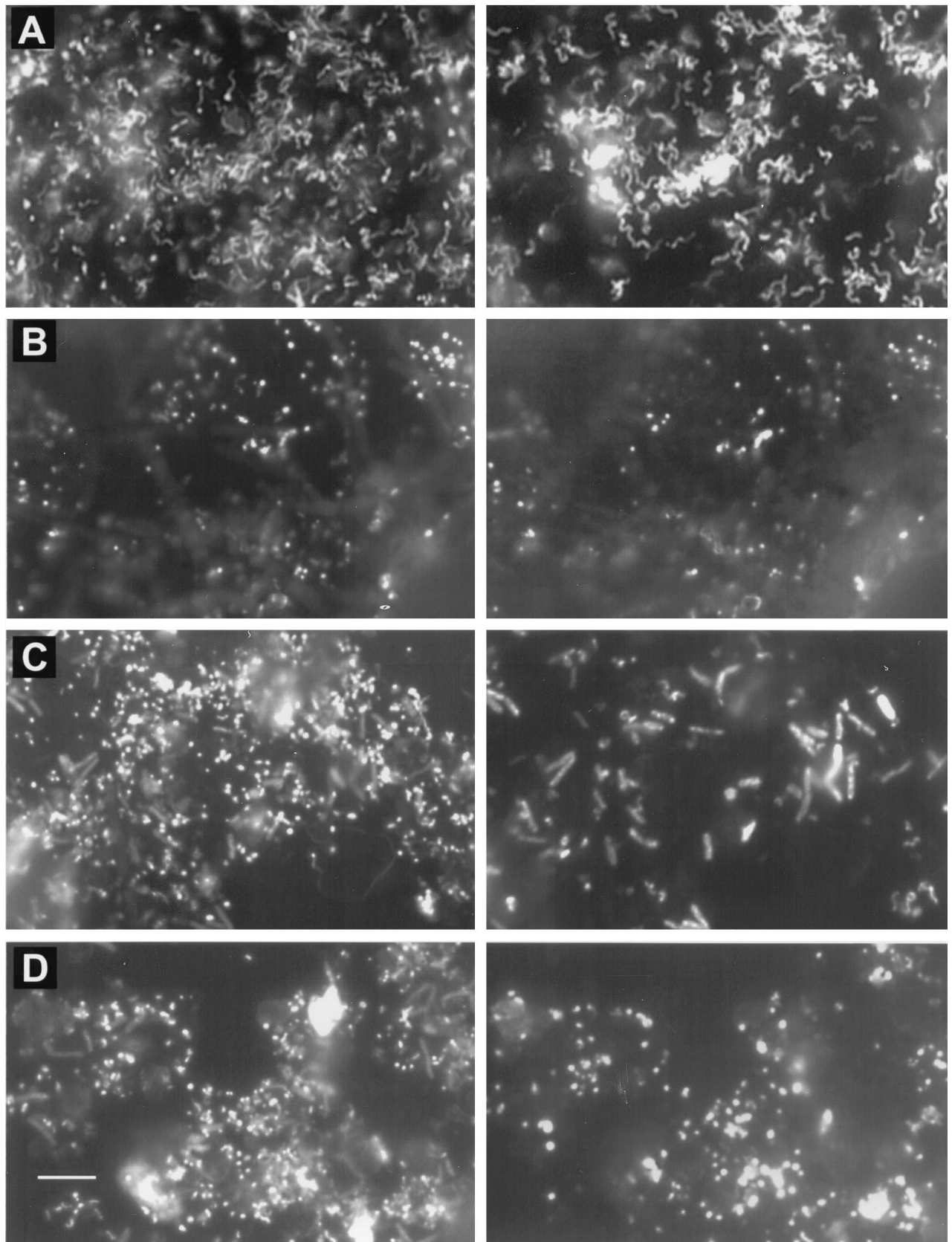


FIG. 5. FISH of Iron Mountain mine samples with various oligonucleotide probes. Horizontally paired images represent the same fields of view. On the left are cells detected by DAPI. On the right is the corresponding view of cells detected with Cy3-labeled probes. (A) Spirilla and curved rods detected with probe LF1252 for *Leptospirillum* group III cells in the slump slime from the A-drift. (B) Cocci attached to a crystal in the B-drift slime, detected with probe FER656, which is specific for the "*Ferroplasma*" genus. (C) Large rods and smaller curved rods in the C-drift slime, detected with the *Bacteria*-specific probe EUB338. (D) Pleomorphic cocci present in the C-drift slime as detected with probe TH1187, specific for organisms of the *Thermoplasmatales* order. The size bar in panel D is 10 μm and applies to all panels.

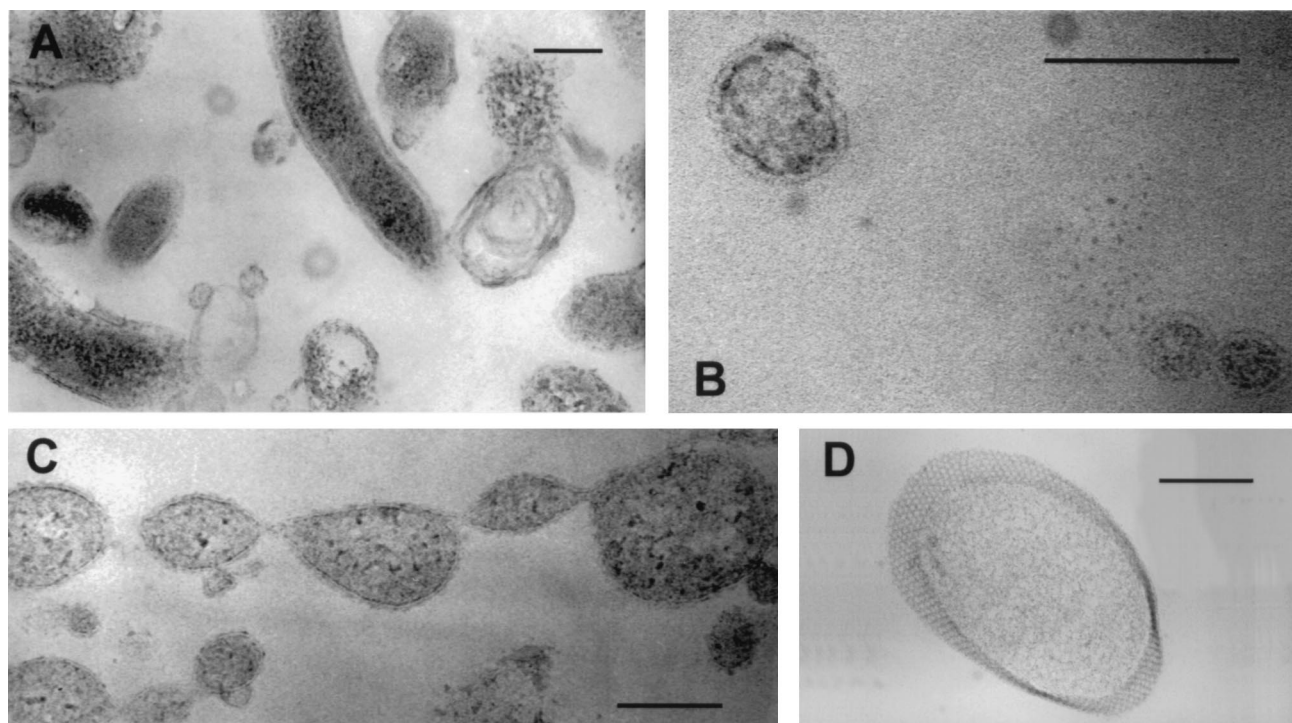


FIG. 6. Transmission electron micrographs of cells in the slump slime (C) and snottite samples (A, B, and D). (A) Range of cell morphologies. (B) Small cell-like structures. (C) Lines of dividing cells. (D) Protein S-layer structure. The size bars in panels A, C, and D are 200 nm. The size bar in panel B is 100 nm.

karyotes were in low abundance and were of protozoan-type morphology.

B-drift communities. The B-drift biofilms (November 1998 and October 1999) were made up mostly of small cocci. Within dense portions of the biofilms, large filaments, presumably fungi, made up significant amounts of the biomass. However, very few of these cells were detected by the probe EUK502 or UNIV1392, indicating that most of the filaments were not active. As the presence of these filaments was restricted mostly to dense portions of the biofilm, they were not enumerated. In both samples of the B-drift slimes, small cocci identified as *Archaea* of the “*Ferroplasma*” genus completely dominated those communities (Fig. 4C and D).

Within the B-drift slimes, cells were detected attached to associated pyrite sediment and transparent crystals (presumably sulfates) (Fig. 5B). Counts of cells attached to sediment particles indicated more diversity than in the associated biofilm (Fig. 4E). Although the cells were still dominated by archaeal “*Ferroplasma*” spp., some 31% of the cells were bacteria, and most of these were *L. ferrooxidans*, as detected with the general *Leptospirillum* probe LF655.

C-drift communities. Two slimes collected from the same region of the C drift in November 1998 and October 1999 contained the most diversity, as measured by cell morphology, of any of the samples investigated. These biofilms comprised mostly densely packed prokaryote cells as well as some filamentous-fungus-type cells. The filaments were detected with the probe EUK502 but were too few to enumerate. The November 1998 sample contained similar proportions of *Bacteria*, mostly *Sulfobacillus* spp., and *Archaea*, mostly of the *Thermoplasmatales* order (Fig. 4G). The October 1999 sample had a microbial community similar to that of the November sample, although there were fewer *Bacteria* and more *Archaea* (Fig. 4H). As in all the samples, the *Archaea* were small, pleomor-

phic cocci (Fig. 5D). Of the *Bacteria*, the large rods were *Sulfobacillus* spp. and the smaller curved rods and spirilla were *L. ferrooxidans* (Fig. 5C). Other bacterial-genus- and species-specific probes were used to further delineate the C-drift slimes. These probes were ACM732 for *Acidimicrobium* spp. and relatives, ACD840 for *Acidiphilium* spp., THC642 for *Acidithiobacillus caldus*, TF539 for *A. ferrooxidans*, and SRB281 for various δ -*Proteobacteria*. However, no cells were detected in the C-drift slimes with these probes.

DISCUSSION

In this study we identify the majority of the prokaryote cells in all the samples using the group-, genus-, and subgenus-specific probes developed for AMD organisms. Thus, we are able to accurately account for these populations at a detailed level. Results show that organisms dominating the low-pH environments are potentially new (not previously detected), although they are related to known acidophiles. These findings significantly advance our understanding of the microbial communities inhabiting this site of extreme AMD production.

On the basis of the level of identification achieved with these probes, only one to three types of organisms dominate each of the environments studied. The most prominent organisms making up these communities are of the order *Thermoplasmatales* (“*Ferroplasma*” spp. in particular), of *Leptospirillum* group III, of *Leptospirillum* group I plus II, *Sulfobacillus* spp., and *Acidimicrobium*-related spp.

The communities analyzed were in direct contact with pyrite or ferrous-iron-rich solutions that interact with the pyrite-dominated ore. Thus, all organisms have the potential to affect pyrite dissolution if they oxidize iron (and, to a lesser extent, if they oxidize sulfur or organic carbon derived from the autotrophs). Most of the cells contain rRNA levels that permit

detection by FISH. This circumstance suggests that cells in these environments are metabolically active rather than dormant or resting.

Ferric ions released by microbial iron oxidation are reduced by oxidation of sulfide groups at the pyrite surface (26). The high ferrous iron/ferric iron ratio is not indicative of low iron oxidation in the mine solutions but rather indicates that the rate of pyrite oxidation is limited by the rate of chemical- and microbe-mediated iron oxidation. Based on the total iron discharged and the amount of pyrite dissolution occurring at the mine (results not shown), we calculate that the iron in solution is reoxidized approximately 14 times along the flow path. Hence, cyclic iron redox reactions, presumably facilitated by microbial oxidations, occur in the mine solutions.

Details of important metabolic transformations are lacking for most of the organisms detected. In particular, *Leptospirillum* group III organisms are not yet cultured and "*Ferroplasma*" spp. from the mine have only recently been isolated (14). However, some of the main physiological characteristics are known for these or related organisms. In this discussion we speculate as to the ecological and physiological roles of important taxonomic groups to AMD production. This speculation can be appropriate when species of a group have common and well-defined traits. For example, all known *Leptospirillum* spp. are chemolithoautotrophs that gain energy by iron oxidation.

Leptospirillum group III organisms dominate the A-drift slump slime and snottite biofilms. Cultures representing group III sequences have not been obtained. However, organisms of *Leptospirillum* groups I and II are autotrophic, oxidize iron for energy (5, 30), and have optimum growth temperatures of 26 to 30°C (group I) and 30 to 40°C (group II) (18). Due to the dominance of *Leptospirillum* group III organisms in the slump slime and snottite, we speculate that the major physiological trait there is iron oxidation.

Acidimicrobium-related cells are present in the slump slime and snottite environments. *Acidimicrobium* and "*Ferromicrobium*" species isolated from other acidophilic environments are iron-oxidizing, heterotrophic bacteria (4, 10). The source of organic carbon for these types of cells in the biofilms is most likely from the slime-associated biomass. It has been suggested that heterotrophic growth of "*Ferromicrobium acidophilus*" removes dissolved organic carbon inhibitory to coexisting autotrophs (4), and that may be a role of the organisms detected here.

Downstream from the A-drift slump, the water surface slime is dominated by *Leptospirillum* group I- and II-type organisms. There are differences in the environments of the water surface biofilm and the slump region. Extremes of temperature and conductivity (higher and lower) occur at the slump (Fig. 3). Physiological differences between the different *Leptospirillum* groups, such as growth temperature optimum and tolerance to ferric ion (18, 31), could cause the microbial-community differences detected in these environments. The presence of both the ferric iron sulfate jarosite and the mixed ferric iron-ferrous iron sulfate voltaite suggests that the redox states of solutions in the slump slime are also variable. Specific environments such as these may favor one *Leptospirillum* group over another.

Archaea of the *Thermoplasmales* order make up a significant proportion of DNA sequences obtained from a snottite sample (7). We suspect that the small cocci detected by DAPI in the slump slime and snottite, but not detected by any probes used here, are the source of the *Thermoplasmales* sequences. TEM data suggest that these samples contain many round cell-like structures (Fig. 6A to C). These are present as separate entities and as buds on larger cells. A subset of larger cells have proteinaceous S layers (Fig. 6D). These features, plus the pres-

ence of only a single membrane bounding the cytoplasm and the pleomorphic cell morphology, support the sequence-based suggestion that these organisms belong to the *Thermoplasmales* order (35). The nature of these small cells is of interest, as many are smaller than the proposed lower limit for autonomous cellular life, which is argued to be in the range of 200 to 250 nm (1). Small cells have been detected in other environments (23, 33), and one explanation for these in the slump slime and snottite is that they are resting cells with low rRNA contents.

Slime streamer biofilms examined from both the B and C drifts contain eukaryote filaments. These filaments possibly increase the integrity of the submerged biofilms in the flowing water. Cells of the "*Ferroplasma*" genus dominate the B-drift slime streamer. This is a seemingly stable population based upon analysis of the November 1998 and October 1999 samples and of other samples taken in February and May 1999 (results not shown). Throughout the study period, the B-drift site is marked by stable conditions (conductivity, pH, and temperature) (Fig. 3), and this stability likely explains the stability of the microbial community. Similar conditions prevailed during a previous study period, when *Archaea*, presumably of the genus "*Ferroplasma*," also dominated the site (15).

Archaea of the genus "*Ferroplasma*" are iron-oxidizing hyperacidophiles (14, 21) and "*Ferroplasma acidarmanus*" is a mine isolate with growth optimums for temperature and pH of 45°C and 1.2, respectively (14). Iron oxidation is inferred to be a major microbial transformation in environments where *Ferroplasma* spp. are important community members, such as in the B-drift slime streamers (14). It appears that the *Archaea* are more competitive at the moderate temperatures and lower pHs found in the B and C drifts (October 1999) (Fig. 3). Thus, in view of their abundance and known physiology, we hypothesize that dissolution mediated by the *Archaea* contributes to the lower-pH environments at the mine.

Iron oxidation is likely a major mechanism of microbial energy generation in these low-pH (0.5 to 1.0) environments. Previous characterization of the chemolithotrophic iron oxidation metabolic pathway is restricted mostly to investigations of *A. ferrooxidans*. This organism is not of principal importance to the pyrite dissolution at Iron Mountain and may be relevant only to iron oxidation that occurs downstream from the dissolution process (15). However, chemolithotrophic iron oxidation is polyphyletic across and within the prokaryotic domains (5, 25). Moreover, spectroscopic measurements of proteins extracted from a range of acidophilic iron-oxidizing bacteria and archaea suggest that mechanisms are diverse (5). Therefore, it is of major importance to investigate iron-oxidizing pathways of organisms that are relevant to AMD production, such as that found in the dominant organisms detected in this study.

The C-drift slime streamer population is distinct from that in the B drift. This community has a larger bacterial component and is dominated by *Sulfobacillus* spp., by *Thermoplasmales* mostly of the genus "*Ferroplasma*," and to a lesser extent by *L. ferrooxidans* spp. (Fig. 4G and H). This environment generally has a slightly higher pH, higher temperatures, and lower conductivity than those of the B drift (Fig. 3). In the C-drift community, reciprocal fluctuations of *Sulfobacillus* and "*Ferroplasma*" spp. coincide with changes in environmental conditions. It appears the *Sulfobacillus* spp. are better adapted to the higher-temperature and slightly higher-pH conditions. These microbial-community changes may reflect temperature and pH growth optimums of the *Sulfobacillus* and *Ferroplasma* spp.

Sulfobacillus spp. have not been isolated from the mine. However, isolates of *Sulfobacillus* spp. are chemolithotrophs

that can use reduced sulfur or iron compounds as an energy source and show mixotrophic and autotrophic growth (20). Typically their temperature optimum is $\sim 50^{\circ}\text{C}$, and their pH optimum is ~ 2.0 (12). Due to the close phylogenetic relationship of organisms detected with SUL228 (6), these cells in the C drift are likely capable of iron and sulfur oxidation. The C drift is a prominent location within the mine, and there is the potential of sulfur-oxidizing organisms facilitating pyrite dissolution there. Our ongoing experiments indicate that the role sulfur-oxidizing organisms play in enhancing sulfide mineral dissolution is not certain (M. M. McGuire, K. J. Edwards, J. F. Banfield, and R. J. Hamers, submitted for publication).

Most communities studied here are possibly more dominated by iron than they are by sulfur-oxidizing species, compared to communities reported (by nonmolecular methods) to exist at higher pHs (28). A recent study of pyrite surface chemistry during dissolution suggests increased sulfur accumulations on pyrite surfaces as pH and temperature increase (8). It is possible that the higher temperature and pH in the C drift correlate with more bioavailable intermediate sulfur compounds, thus explaining the increased diversity detected in the C drift.

Another important microenvironment for production of AMD is that of pyrite-attached cells. It is thought that the use of different mechanisms of microbial sulfide dissolution, such as direct and indirect mechanisms (34), influences cell attachment to the ore. Therefore, the type of mechanism utilized by particular organisms may affect attached and nonattached community compositions. To investigate this, we compared the slime streamer microbial community with the community of cells attached to pyrite sediment particles in B-drift samples (Fig. 4D and E). "*Ferropasma*" spp. dominate both the slime and the sediment-attached cells. However, more diversity is present in the sediment-attached cells, where *L. ferrooxidans* makes up a greater proportion. However, it is difficult to draw conclusions from these results. It is known that temperature, ionic strength, pH, and likely redox conditions change with depth into the pyrite accumulations on the drift floors. Further investigations are required to understand the population character in more sediment-dominated settings.

Attachment of cells to ferrous iron sulfate crystals may be significant to the cycling of iron and sulfur at the mine. Preferential attachment of cells to crystals is observed in the slump slime and in the B- and C-drift slimes. Evaporative sulfosalts cover portions of the mine tunnel walls and ceiling, and these occasionally slump into the sediment. These can make up significant fractions of floor accumulations (up to approximately 25%) and are an important source of acidity (27). Under the appropriate conditions, microorganisms may preferentially attach to the more reduced sulfosalts and use them as a source of reduced iron.

Conclusions. The majority of the organisms detected at the mine are either uncultured or recently described species. Given that most of these are inferred to oxidize iron, species of *Ferropasma*, *Leptospirillum* groups II and III, *Sulfobacillus*, and to a lesser extent *Acidimicrobium* are likely to be the most important organisms to AMD production at the Iron Mountain mine. Future studies concerned with understanding details of the microbial role in AMD generation or bioleaching (9) should focus on these relevant organisms. Our results implicate these organisms as important contributors to the oxidative portion of the terrestrial sulfur and iron geochemical cycles.

Few organism types dominate the communities examined here. This is typical of communities that face physically and chemically restricting environments (3), such as the severe conditions occurring at the Iron Mountain mine. Within the

environments studied, distinct microbial-community compositions are detected, and these reflect environmental and geochemical differences. We suggest that the restricted types of available electron donors and acceptors and the extreme nature of these highly acidic, metal-rich environments are primary factors shaping the microbial ecology here.

ACKNOWLEDGMENTS

Thanks are expressed to Thomas Gihring and Katrina Edwards for invaluable suggestions. Steve Smriga is also thanked for help with sample collection. The expertise of Alice Dohnalkova, in the preparation of samples for electron microscopy, is appreciated. Assistance from Bob Hamers is also gratefully acknowledged.

This project received NSF support via a supplement to grant CHE 9521731, as well as support from NSF CHE 9807598.

REFERENCES

- Adams, M. W. W. 1999. The influence of environment and metabolic capacity on the size of a microorganism, p. 74–80. *In* Size limits of very small microorganisms. National Academy Press, Washington, D.C.
- Amann, R. I., L. Krumholz, and D. A. Stahl. 1990. Fluorescent-oligonucleotide probing of whole cells for determinative, phylogenetic, and environmental studies in microbiology. *J. Bacteriol.* **172**:762–770.
- Atlas, R. M., A. Horowitz, M. Krichevsky, and A. K. Bej. 1991. Response of microbial-populations to environmental disturbance. *Microb. Ecol.* **22**:249–256.
- Bacelar-Nicolau, P., and D. B. Johnson. 1999. Leaching of pyrite by acidophilic heterotrophic iron-oxidizing bacteria in pure and mixed cultures. *Appl. Environ. Microbiol.* **65**:585–590.
- Blake, R. C., E. A. Shute, M. M. Greenwood, G. H. Spencer, and W. J. Ingledew. 1993. Enzymes of aerobic respiration on iron. *FEMS Microbiol. Rev.* **11**:9–18.
- Bond, P. L., and J. F. Banfield. Design and performance of rRNA targeted oligonucleotide probes for in situ detection and phylogenetic identification of microorganisms inhabiting acid mine drainage environments. *Microb. Ecol.*, in press.
- Bond, P. L., S. P. Smriga, and J. F. Banfield. 2000. Phylogeny of microorganisms populating a thick, subaerial, predominantly lithotrophic biofilm at an extreme acid mine drainage site. *Appl. Environ. Microbiol.* **66**:3842–3849.
- Boogerd, F. C., C. Vandenberg, T. Stoelwinder, P. Bos, and J. G. Kuennen. 1991. Relative contributions of biological and chemical-reactions to the overall rate of pyrite oxidation at temperatures between 30-degrees-C and 70-degrees-C. *Biotechnol. Bioeng.* **38**:109–115.
- Bosecker, K. 1997. Bioleaching: metal solubilization by microorganisms. *FEMS Microbiol. Rev.* **20**:591–604.
- Bridge, T. A. M., and D. B. Johnson. 1998. Reduction of soluble iron and reductive dissolution of ferric iron-containing minerals by moderately thermophilic iron-oxidizing bacteria. *Appl. Environ. Microbiol.* **64**:2181–2186.
- Clark, D. A., and P. R. Norris. 1996. *Acidimicrobium ferrooxidans* gen. nov., sp. nov.—mixed-culture ferrous iron oxidation with *Sulfobacillus* species. *Microbiology* **142**:785–790.
- Duffresne, S., J. Bousquet, M. Boissinot, and R. Guay. 1996. *Sulfobacillus disulfidooxidans* sp. nov., a new acidophilic, disulfide-oxidizing, gram-positive, spore-forming bacterium. *Int. J. Syst. Bacteriol.* **46**:1056–1064.
- Edwards, K. J., P. L. Bond, and J. F. Banfield. 2000. Characteristics of attachment and growth of *Thiobacillus caldus* on sulfide minerals: a chemotactic response to sulfur minerals? *Environ. Microbiol.* **2**:324–332.
- Edwards, K. J., P. L. Bond, T. M. Gihring, and J. F. Banfield. 2000. An archaeal iron-oxidizing extreme acidophile important in acid mine drainage. *Science* **287**:1796–1799.
- Edwards, K. J., T. M. Gihring, and J. F. Banfield. 1999. Seasonal variations in microbial populations and environmental conditions in an extreme acid mine drainage environment. *Appl. Environ. Microbiol.* **65**:3627–3632.
- Edwards, K. J., B. M. Goebel, T. M. Rodgers, M. O. Schrenk, T. M. Gihring, M. M. Cardona, B. Hu, M. M. McGuire, R. J. Hamers, N. R. Pace, and J. F. Banfield. 1999. Geomicrobiology of pyrite (FeS₂) dissolution: case study at Iron Mountain, California. *Geomicrobiol. J.* **16**:155–179.
- Edwards, K. J., M. O. Schrenk, R. Hamers, and J. F. Banfield. 1998. Microbial oxidation of pyrite: experiments using microorganisms from an extreme acidic environment. *Am. Mineral.* **83**:1444–1453.
- Goebel, B. M., and E. Stackebrandt. 1994. The biotechnological importance of molecular biodiversity studies for metal bioleaching, p. 259–273. *In* F. G. Priest, A. Ramos-Cormenzana, and B. J. Tindall (ed.), *Bacterial diversity and systematics*, vol. VIII. Plenum Press, New York, N.Y.
- Goebel, B. M., and E. Stackebrandt. 1994. Cultural and phylogenetic analysis of mixed microbial populations found in natural and commercial bioleaching environments. *Appl. Environ. Microbiol.* **60**:1614–1621.

20. Golovacheva, R. S., and G. I. Karavaiko. 1978. A new genus of thermophilic spore-forming bacteria, *Sulfobacillus*. *Microbiology* **47**:658–664.
21. Golyshina, O. V., T. A. Pivovarova, G. I. Karavaiko, T. F. Kondrat'eva, E. R. B. Moore, W. R. Abraham, H. Lunsdorf, K. N. Timmis, M. M. Yakimov, and P. N. Golyshin. 2000. *Ferroplasma acidiphilum* gen. nov., sp. nov., an acidophilic, autotrophic, ferrous-iron-oxidizing, cell-wall-lacking, mesophilic member of the *Ferroplasmaceae* fam. nov., comprising a distinct lineage of the Archaea. *Int. J. Syst. Evol. Microbiol.* **50**:997–1006.
22. Johnson, D. B. 1998. Biodiversity and ecology of acidophilic microorganisms. *FEMS Microbiol. Ecol.* **27**:307–317.
23. Kajander, E. O., and N. Ciftcioglu. 1998. Nanobacteria: an alternative mechanism for pathogenic intra- and extracellular calcification and stone formation. *Proc. Natl. Acad. Sci. USA* **95**:8274–8279.
24. Kelly, D. P., and A. P. Wood. 2000. Reclassification of some species of *Thiobacillus* to the newly designated genera *Acidithiobacillus* gen. nov., *Halothiobacillus* gen. nov. and *Thermithiobacillus* gen. nov. *Int. J. Syst. Evol. Microbiol.* **50**:511–516.
25. Lane, D. J., A. P. Harrison, D. Stahl, B. Pace, S. J. Giovannoni, G. J. Olsen, and N. R. Pace. 1992. Evolutionary relationships among sulfur-oxidizing and iron-oxidizing eubacteria. *J. Bacteriol.* **174**:269–278.
26. Moses, C. O., D. K. Nordstrom, J. S. Herman, and A. L. Mills. 1987. Aqueous pyrite oxidation by dissolved-oxygen and by ferric iron. *Geochim. Cosmochim. Acta* **51**:1561–1571.
27. Nordstrom, D. K., and C. N. Alpers. 1999. Negative pH, effluorescent mineralogy, and consequences for environmental restoration at the Iron Mountain Superfund site, California. *Proc. Natl. Acad. Sci. USA* **96**:3455–3462.
28. Nordstrom, D. K., and G. Southam. 1997. Geomicrobiology of sulfide mineral oxidation, p. 361–390. *In* J. F. Banfield and K. H. Nealson (ed.), *Geomicrobiology: interactions between microbes and minerals*, vol. 35. Mineralogical Society of America, Washington, D.C.
29. Olsen, G. J., D. J. Lane, S. J. Giovannoni, N. R. Pace, and D. A. Stahl. 1986. Microbial ecology and evolution: a ribosomal RNA approach. *Annu. Rev. Microbiol.* **40**:337–365.
30. Pivovarova, T. A., G. E. Markosyan, and G. I. Karavaiko. 1981. The auxotrophic growth of *Leptospirillum ferrooxidans*. *Microbiology* **50**:339–344.
31. Rawlings, D. E., H. Tributsch, and G. S. Hansford. 1999. Reasons why '*Leptospirillum*'-like species rather than *Thiobacillus ferrooxidans* are the dominant iron-oxidizing bacteria in many commercial processes for the biooxidation of pyrite and related ores. *Microbiology* **145**:5–13.
32. Rodgers, T. M. 1996. Bacterial diversity in acid mine drainage from Iron Mt., Shasta County, California: a 16S ribosomal RNA approach. Masters thesis. University of Wisconsin, Madison.
33. Roszak, D. B., and R. R. Colwell. 1987. Survival strategies of bacteria in the natural environment. *Microbiol. Rev.* **51**:365–379.
34. Sand, W., T. Gerke, R. Hallmann, and A. Schippers. 1995. Sulfur chemistry, biofilm, and the (in)direct attack mechanism—a critical-evaluation of bacterial leaching. *Appl. Microbiol. Biotechnol.* **43**:961–966.
35. Schleper, C., G. Puchler, I. Holz, A. Gambacorta, D. Janekovic, U. Santarius, H. P. Klenk, and W. Zillig. 1995. *Picrophilus* gen. nov., fam. nov.: a novel aerobic, heterotrophic, thermoacidophilic genus and family comprising archaea capable of growth around pH 0. *J. Bacteriol.* **177**:7050–7059.
36. Schrenk, M. O., K. J. Edwards, R. M. Goodman, R. J. Hamers, and J. F. Banfield. 1998. Distribution of *Thiobacillus ferrooxidans* and *Leptospirillum ferrooxidans*—implications for generation of acid mine drainage. *Science* **279**:1519–1522.
37. Stahl, D. A., and R. Amann. 1991. Development and application of nucleic acid probes in bacterial systematics, p. 205–248. *In* E. Stackebrandt and M. Goodfellow (ed.), *Nucleic acid techniques in bacterial systematics*. John Wiley & Sons, Chichester, United Kingdom.
38. Wallner, G., R. Amann, and W. Beisker. 1993. Optimizing fluorescent in situ hybridization with rRNA-targeted oligonucleotide probes for flow cytometric identification of microorganisms. *Cytometry* **14**:136–143.
39. Walton, K. C., and D. B. Johnson. 1992. Microbiological and chemical characteristics of an acidic stream draining a disused copper mine. *Environ. Pollut.* **76**:169–175.